



Static correlations functions and domain walls in glass-forming liquids: The case of a sandwich geometry

Giacomo Gradenigo, Roberto Trozzo, Andrea Cavagna, Tomás S. Grigera, and Paolo Verrocchio

Citation: *J. Chem. Phys.* **138**, 12A509 (2013); doi: 10.1063/1.4771973

View online: <http://dx.doi.org/10.1063/1.4771973>

View Table of Contents: <http://jcp.aip.org/resource/1/JCPSA6/v138/i12>

Published by the [American Institute of Physics](http://www.aip.org).

Additional information on *J. Chem. Phys.*

Journal Homepage: <http://jcp.aip.org/>

Journal Information: http://jcp.aip.org/about/about_the_journal

Top downloads: http://jcp.aip.org/features/most_downloaded

Information for Authors: <http://jcp.aip.org/authors>

ADVERTISEMENT



Goodfellow
metals • ceramics • polymers • composites
70,000 products
450 different materials
small quantities fast

www.goodfellowusa.com

Static correlations functions and domain walls in glass-forming liquids: The case of a sandwich geometry

Giacomo Gradenigo,^{1,2,a)} Roberto Trozzo,¹ Andrea Cavagna,^{1,2} Tomás S. Grigera,^{3,4} and Paolo Verrocchio^{5,6,7}

¹Dipartimento di Fisica, Università Sapienza, P.le Aldo Moro 2, 00185 Roma, Italy

²Istituto Sistemi Complessi (ISC), Consiglio Nazionale delle Ricerche (CNR), UOS Sapienza, Via dei Taurini 19, 00185 Roma, Italy

³Instituto de Investigaciones Fisicoquímicas Teóricas y Aplicadas (INIFTA) and Departamento de Física, Facultad de Ciencias Exactas, Universidad Nacional de La Plata, c.c. 16, suc. 4, 1900 La Plata, Argentina

⁴CONICET La Plata, Consejo Nacional de Investigaciones Científicas y Técnicas, Argentina

⁵Dipartimento di Fisica and Interdisciplinary Laboratory for Computational Physics (LISC), Università di Trento, via Sommarive 14, 38050 Povo, Trento, Italy

⁶Istituto Sistemi Complessi (ISC-CNR), UOS Sapienza, Via dei Taurini 19, 00185 Roma, Italy

⁷Instituto de Biocomputación y Física de Sistemas Complejos (BIFI), Spain

(Received 25 September 2012; accepted 29 November 2012; published online 2 January 2013)

The problem of measuring nontrivial static correlations in deeply supercooled liquids made recently some progress thanks to the introduction of amorphous boundary conditions, in which a set of free particles is subject to the effect of a different set of particles frozen into their (low temperature) equilibrium positions. In this way, one can study the crossover from nonergodic to ergodic phase, as the size of the free region grows and the effect of the confinement fades. Such crossover defines the so-called point-to-set correlation length, which has been measured in a spherical geometry, or cavity. Here, we make further progress in the study of correlations under amorphous boundary conditions by analyzing the equilibrium properties of a glass-forming liquid, confined in a planar (“sandwich”) geometry. The mobile particles are subject to amorphous boundary conditions with the particles in the surrounding walls frozen into their low temperature equilibrium configurations. Compared to the cavity, the sandwich geometry has three main advantages: (i) the width of the sandwich is decoupled from its longitudinal size, making the thermodynamic limit possible; (ii) for very large width, the behaviour off a single wall can be studied; (iii) we can use “anti-parallel” boundary conditions to force a domain wall and measure its excess energy. Our results confirm that amorphous boundary conditions are indeed a very useful new tool in the study of static properties of glass-forming liquids, but also raise some warning about the fact that not all correlation functions that can be calculated in this framework give the same qualitative results. © 2013 American Institute of Physics. [<http://dx.doi.org/10.1063/1.4771973>]

I. INTRODUCTION

The sharp slowdown observed in supercooled liquids at low temperatures has long been conceptually connected to the buildup of structural (static) correlations. Yet, due to the amorphous nature of the excitations, it has proved rather difficult to identify them and to measure their size. For this reason, dynamical correlations^{1–12} were detected much before static ones, and only recently were structural correlations unveiled, using novel techniques.^{13–17}

Among these techniques, numerical simulations with amorphous boundary conditions (ABC), and the related point-to-set correlation length ξ , have proved very fruitful.^{14,18–23} Implementing ABCs is simple, at least in numeric simulations. Consider a set of mobile and another one of frozen particles and let the mobile particles evolve under the influence of the frozen ones, eventually reaching thermodynamic equilibrium. The simplest case is when the frozen particles belong to a single equilibrium configuration surrounding a spherical

cavity of mobile particles, of radius R . It is possible then to define an overlap $q(R)$ and to measure the similarity at the center of the sphere between two configurations. The dependence of the overlap on the linear size R of the cavity yields the correlation length ξ , defined by the crossover at $R \sim \xi$ among the values $q(R) \sim 1$ (almost identical configuration) and $q(R) \sim 0$ (statistically independent configurations).

The original ABC spherical realization can be generalized to different geometries, where the frozen particles do not necessarily form a closed cavity.^{20,21,24} In this work, we study the case of a planar (or “sandwich”) geometry (see Fig. 1). As with the spherical geometry, in the sandwich we can calculate a point-to-set length by studying the sandwich width beyond which the internal mobile particles reach ergodicity. In this respect, our study aims to verify the results obtained in the cavity and test their robustness. In particular, we are interested to check whether or not the anomalous nonexponential behaviour of the point-to-set correlation function at low T observed in the spherical geometry¹⁹ is also found in the sandwich. To check how general is this nonexponential behaviour is important because it is one of the very few

^{a)}Electronic mail: ggradenigo@gmail.com.

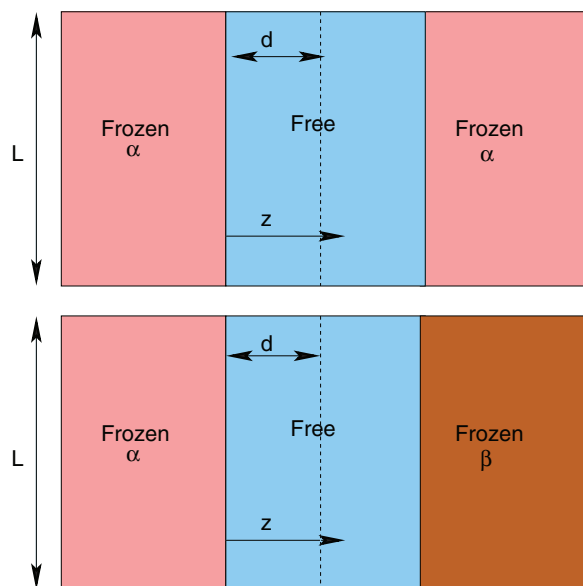


FIG. 1. Cartoon of the sandwich geometry. In the ‘parallel’ (or $\alpha\alpha$) setup (top) both frozen walls are taken from the same equilibrium configuration, while in the ‘anti-parallel’ ($\alpha\beta$) case, they come from different configurations (bottom).

qualitative thermodynamic landmarks of the deeply supercooled phase.

But the sandwich also allowed us to study cases that are out of reach in the cavity. First, in the sandwich the width d and the longitudinal size L are independent parameters, so that we can perform the limit $L \rightarrow \infty$ while the confinement length keeping d finite. This thermodynamic limit is clearly impossible in the cavity. This limit is important, as by increasing the number of mobile particles at constant degree of confinement, we can check whether or not the finite-size crossovers of the correlation functions turn into bona fide transitions.

Second, when the two walls are very far from each other ($d \rightarrow \infty$), we can study the decay of the overlap off a single wall, as a function of the distance z from the wall. This is not strictly impossible in spherical geometry, but in that case one could be exposed to spurious curvature effects that are absent in the sandwich.

Third, in the planar geometry we can use different amorphous boundary conditions on the two sides of the sandwich (Fig. 1, bottom), which is also impossible in the cavity. This sort of ‘‘anti-parallel’’ boundary conditions can be used to force a domain wall in the system, and therefore to measure its excess energy and the stiffness exponent θ . These quantities are crucial in any phenomenological description of the glass transition, so that any new tool able to provide information on these quantities may be helpful.

II. MODEL AND SIMULATION DETAILS

We study the soft-sphere binary mixture,²⁵ a simple model of supercooled liquids widely studied before, and in which the point-to-set correlation has been computed using a cavity. We use the accelerated Swap Monte Carlo algorithm²⁶

to thermalize the system at temperatures as low as possible. We run simulations at $T = 0.482, 0.350, 0.246, 0.202$. The first two temperatures correspond to the high-temperature liquid, the third is near the ‘‘onset’’ or ‘‘landscape-influenced’’ temperature²⁷ and the lowest temperature lies in the supercooled regime, in which the landscape is dominated by minima of the potential energy rather than saddle points.

The confined system is generated from configurations taken from equilibrated periodic-boundary-conditions runs. These runs were done with density $\rho = 1$ and box sizes $L = 16$ and $L = 25.3$. At each temperature we then chose several (from 16 to 24) configurations and artificially froze in their equilibrium positions all but M particles contained within a region of the simulation box in the shape of a box of size $2d \times L^2$ (we measure d along the z axis).

In order to keep the density fixed within the region of mobile particles, it is a standard practice to place virtual walls at the border of such mobile regions. What we do is the following: taking configurations of the liquid system, we place a hard wall potential enclosing the free particles. This destroys translational invariance along the z axis, but not along the xy planes, creating a sandwich of mobile particles surrounded by two infinite walls of frozen liquid.

The main observable we consider is the infinite time limit of the local density-density correlations. More precisely, we define the overlap $q(z; d)$, as follows: we partition the simulation box in many small cubic boxes of side ℓ , such that the probability of finding more than one particle in a single box is negligible. If n_i is the number of particles in box i , then

$$q(z; d) = \lim_{t \rightarrow \infty} \frac{1}{\ell^3 N_i} \sum_{i \in v} \langle n_i(t_0) n_i(t_0 + t) \rangle, \quad (1)$$

where the sum runs over all boxes that lie on a plane parallel to the xy plane at the given distance z from one reference wall, N_i is the number of boxes in each of those planes, and $\langle \dots \rangle$ indicates a thermal average. Normalization is such that the overlap of two identical configurations is 1 on average, while for totally uncorrelated configurations $q = q_0 \equiv \ell^3 = 0.062876$.

III. DIFFERENT STATIC LENGTHSCALES

In this section, we study the overlap, Eq. (1), in the sandwich geometry described above, in which mobile particles are confined within a volume $2dL^2$ by two walls made of frozen particles (top scheme in Fig. 1). In our description, d is the half-width of the sandwich; we believe this is the correct variable to compare our results (especially lengthscales) with the spherical cavity case. It is important to note that both walls are made from particles taken from the same equilibrated configuration.

In general, the overlap is a measure of the nonergodicity of the mobile part of the sandwich due to the frozen boundary conditions. When the overlap is nonzero (more precisely: larger than its ergodic value q_0) it means that the phase space available to the particles’ relaxation is reduced by the confinement. It is therefore natural to ask how ‘‘far away’’ the walls need to be so that ergodicity is restored. In the case of the sandwich, this question can be asked in two ways:

1. How big must the wall separation be so that the liquid inside behaves like the bulk?
2. Given a very large (or infinite) cavity, how far from the walls must one look so that the liquid behaves like in the bulk?

The first question implies that one is observing the overlap as a function of d at some reference position within the sandwich (typically at the center, since influence of the walls very near the interface is always expected). In the second question, one considers the overlap as a function of z at fixed, very large d . As we shall see, the two questions have qualitatively and quantitatively different answers.

A. Point-to-set correlation length

We first study the decay of the overlap following the point-to-set prescription, i.e., measuring the overlap at the center of the sandwich ($z = d$) and varying the distance d between the walls (by symmetry, we can actually average the overlap over the whole central plane). We call this point-to-set overlap, computed at the central plane $q_c(d)$. The behaviour of this quantity is shown in Fig. 2 for four different temperatures. The scale of decay of this function defines the point-to-set correlation length ξ .

A notable feature of $q_c(d)$ is that its decay crosses over from simple exponential at high temperatures to nonexponential at low temperatures. In the low T phase a simple exponential fit does a very bad job, while the curves can be fitted via a “compressed exponential” form,

$$q_c(d) = \Omega \exp[-(d/\xi)^\zeta] + q_0, \quad (2)$$

where the anomaly exponent ζ measures the deviation from exponentiality. This specific form is by no means the only one capable of capturing the nonexponential shape. The relevant point is that such nonexponential behaviour is present, and that it is useful to have a scalar parameter (in this case ζ) to quantify it.

At high temperatures a semilog plot shows that the curves are reasonably exponential, so in order to avoid overfitting we fix $\zeta = 1$ and we fit the data to a pure exponential. On the other hand, at low temperatures there is a clear deviation from

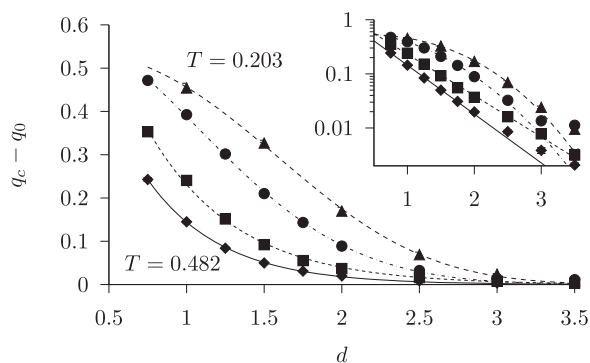


FIG. 2. Overlap at the center of the sandwich vs. sandwich half-width d in the parallel setup for (from left to right) $T = 0.482, 0.350, 0.246, 0.202$. Lines are exponential or compressed-exponential fits (see text). (Inset) Same data in semilog plot.

TABLE I. Point-to-set correlation length ξ , and anomaly exponent ζ , from a fit of Eq. (19); penetration length λ , from a fit of Eq. (20); and excess energy decay lengthscale l , from a fit of Eq. (21). At the highest temperature the value of l has large uncertainty as we have very few nonzero values of ΔE .

T	ξ	ζ	λ	l
0.482	0.48	1	0.47	0.15
0.350	0.56	1	0.56	0.33
0.246	1.50	2.1	0.69	0.43
0.202	2.00	2.7	0.79	0.50

exponentiality (inset of Fig. 2), so that the nonexponential fit (Eq. (2)) is used. At the lowest T we obtain $\zeta = 2.7 \pm 0.2$ (see Table I for all values of ζ).

This progressive sharpening of the decay at low temperatures (growing of the anomaly exponent) is also found in the spherical cavity,¹⁹ but the numerical value of the exponent ζ is different (lower) in the sandwich case. Thus, the geometry of the system may influence the strength of the exponential/nonexponential crossover but the existence of the crossover itself seems not to depend on the geometry and it is therefore a robust result.

B. Penetration length

We now consider the decay of the overlap off one single wall. It is clear from Fig. 3 that for a large enough value of the sandwich width d , the overlap has enough room to decay to its liquid value q_0 at the central plane, at all temperatures. Therefore, the decay of the overlap, $q(z, d \gg \xi)$, as a function of the distance z from one of the two walls, is perfectly equivalent to the decay of the overlap from a single wall in a semi-infinite geometry. We call this quantity simply $q(z)$.

Figure 4 shows the behaviour of $q(z)$ focusing on one single wall. The first feature that we notice, in comparison with the point-to-set correlation function, is that at all temperatures data are well fitted with a simple exponential,

$$q(z) = \exp[-z/\lambda] + q_0, \quad (3)$$

where λ is the penetration length. Independently from the fit quality, the pure exponential behaviour is evident from the semilog plot (inset of Fig. 4). This result is in agreement

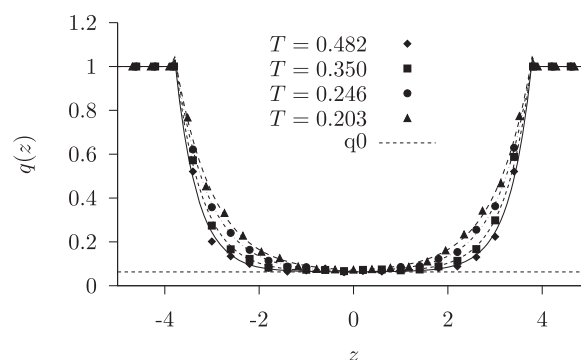


FIG. 3. Overlap in the parallel setup as a function of z for a sandwich of half-width $d = 4$ at several temperatures. The free region is wide enough that the overlap can reach its bulk value q_0 near the center.

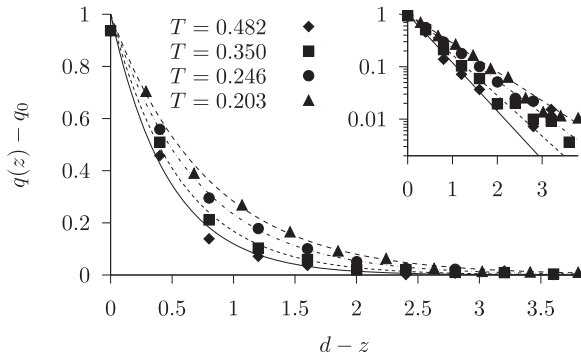


FIG. 4. Overlap vs. $d - z$ (distance from wall) at fixed d (same data as Fig. 3) with pure exponential fits. (Inset) Same data in semilog scale.

with the results obtained with a single wall in Refs. 20 and 21: an exponential decay at all temperatures with no sign of crossover to nonexponentiality. This feature is a remarkable difference with respect to the nonexponential point-to-set correlation $q_c(d)$. Such difference is perhaps not surprising: the two quantities are conceptually not the same, as we shall argue in Sec. IV.

Apart from the functional form of the decay, another difference that we immediately notice is that the penetration length λ seems to be smaller than the correlation length ξ . We will return to this in Sec. VI.

IV. MOSAIC IN THE SANDWICH

A. Naive argument

We have shown in Subsection III A that the decay of the overlap in the sandwich has the same exponential/super-exponential crossover with temperature that is observed in the spherical geometry. Such anomalous nonexponential behaviour at low T was explained in Ref. 19 by using a generalization of the random first order transition (RFOT) framework. In this section we will show that, at least at the naïve level, the same RFOT arguments that hold in the cavity can be also applied to the present sandwich geometry.

The basic idea of RFOT is that the relaxation of a confined system is regulated by trade-off between a cost and a gain of exploring states other from the one fixed into the amorphous boundary conditions. The cost is the free energy the system has to pay to form an interface when it changes state, whereas the gain is the entropic surplus the system enjoys by changing state.^{28–30} The slight complication of the sandwich is that one must be careful to take account of its anisotropic geometry. Unless we are at some very specific value of the parameters (that we shall discuss later), it seems reasonable to assume that the rearrangement of the mobile part of the sandwich happens independently within uncorrelated regions, whose longitudinal size is larger than the correlation length ξ . If we call A and B two such regions, we are saying that

$$\mathcal{Z}_{A+B} \approx \mathcal{Z}_A \mathcal{Z}_B. \quad (4)$$

This means that the overlap of the mobile particles will be basically a longitudinal average of the overlaps of such un-

correlated regions,

$$q_c(d, L) = \frac{1}{n} \sum_{r=1}^n q_c^{(r)}(d), \quad (5)$$

where n is the number of uncorrelated regions along the sandwich.

If we accept this, then the RFOT argument can be run over one independent region of longitudinal size $\sim \xi$, and of width $\sim d$. Exactly as in the cavity, the entropic gain is (all relations are given in the three-dimensional case)

$$\Delta F_{\text{gain}} \sim T \Sigma \xi^2 d. \quad (6)$$

The surface tension cost, however, is trickier than in the cavity. On one hand, we know that it must scale like a length to the power θ , the stiffness exponent. On the other hand, we also expect from extensivity reasons that this cost must scale like the longitudinal size of the rearranging region to the power $d - 1 = 2$: surely, if we build a super-sandwich by putting many sandwiches aside, the total cost must be additive. We can encapsulate these two requirements by writing

$$\Delta F_{\text{cost}} \sim Y d^\theta f(d/\xi), \quad (7)$$

where $f(d/\xi)$ is a scaling function that, due to extensivity, must obey the relation

$$f(d/\xi) \sim \xi^2/d^2, \quad \xi \gg 1. \quad (8)$$

In the end, we get

$$\Delta F_{\text{cost}} \sim Y \xi^2 d^{\theta-2}. \quad (9)$$

As usual in the RFOT argument, we obtain the correlation length, i.e., the lengthscale at which the overlap decays to zero, as the value of d where the two contributions balance, $\Delta F_{\text{gain}} \sim \Delta F_{\text{cost}}$. This yields

$$d_{\text{RFOT}} \sim \left(\frac{Y}{T \Sigma} \right)^{\frac{1}{3-\theta}}. \quad (10)$$

This is the same prediction as RFOT gives in a cavity geometry. This sharp RFOT scenario should then be smoothed by including the surface tension fluctuations, following Ref. 19. In this way, one gets a $q_c(d)$ that decays on a scale d_{RFOT} , and whose decay is sharper and sharper (larger exponent ζ) the lower the temperature, in agreement with what we find numerically. In this context, the point-to-set correlation length ξ must be identified with the RFOT lengthscale d_{RFOT} ,

$$\xi \sim d_{\text{RFOT}}. \quad (11)$$

Note that, at the level of this naïve treatment, the difference between the two walls vs. the single wall geometry, and therefore the difference between $q_c(d)$ and $q(z)$, is quite clear. In the single wall case, the entropic gain is infinite, as flipping the entire semi-plane is an advantage over any interface energy. So, we do not expect any trade-off in that case. However, even in the single wall geometry, the best distance λ where to locate the interface will be nontrivial, since it may be entropically inconvenient for the system to squeeze the interface too close to the wall.³¹ But it will be the entropy of the rough interface, not that of the bulk, to matter. For this reason, we do not expect the growth of λ to be regulated by a classic RFOT

trade-off, while we do expect so for the point-to-set length ξ . No surprise, then, that the two quantities are different.

B. Sharpening in the thermodynamic limit?

As we argued before, an advantage of the sandwich geometry over the cavity is that one can tune the width d and the longitudinal size L independently. This means that (at least in principle) in the sandwich one can perform the thermodynamic limit $L \rightarrow \infty$ at fixed d . However, because of the statistical factorization hypothesis (Eq. (4)), the longitudinal size L plays no role at all in the RFOT argument. In general, this is not necessarily correct. It has been argued in Ref. 32 that, depending on the specific system's geometry and on the dimensionality, the limit $L \rightarrow \infty$ can actually turn the $q_c(d)$ smooth decay with d , into a bona fide, sharp transition at $d = d_{\text{PTS}}$, even at $T > T_k$. We will only sketch the argument here.

What we have disregarded above is the interaction between the different rearranging regions in the mobile part. Consider two neighbouring regions, A and B , and ask which is the propensity of A to decorrelate from its initial state. Clearly, this depends on the frozen boundaries enclosing A , but also on the state of the neighbouring particles in B .^{33,34} The state of B may favour or not the ergodization of A ,^{33,34} and one should take into account this interaction. According to the theoretical scenario of Ref. 32, it turns out that exactly at the transition point $d = d_{\text{RFOT}}$, this longitudinal interaction can make the sandwich long-range correlated along the longitudinal plane. This phenomenon would work in the direction of making the transition between IN and OUT states sharper and sharper. However, in Ref. 32 it is also remarked that such transition is smoothed by the presence of the disorder (disorder is generated by the surface tension fluctuations along the sandwich) and that this has the effect to suppress the transition in a $d = 3$ sandwich, which is our case. Therefore, one should not expect any particular effect when increasing L (the transition would not be suppressed in a $d = 4$ sandwich, nor in a $d = 3$ system with randomly frozen particles, though — see Ref. 34).

We report the overlap $q_c(d, L)$ for two different sizes, $L = 16$ and $L = 25$, in Fig. 5. Indeed we do not find any evidence of a sharpening of the decay of for larger L , which confirms the expectation above. For a three-dimensional sand-

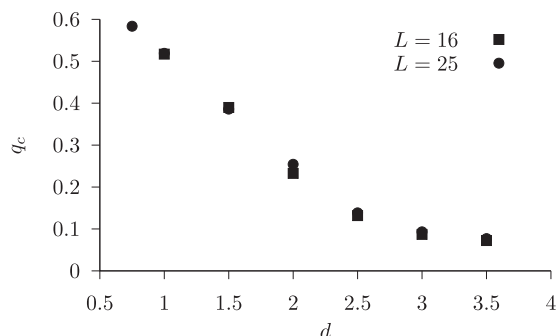


FIG. 5. Overlap at center vs. sandwich half-width d at $T = 0.203$ and two values of L .

wich, thus, the naïve RFOT argument provided at the beginning of this section is probably good enough.

V. “ANTI-PARALLEL” BOUNDARY CONDITIONS

We now turn to the study of the excess energy produced by forcing an interface in the mobile part of the sandwich. To do this we use “anti-parallel” boundary conditions: we freeze particles on one wall in a configuration α , and those on the other wall in a different configuration β (see Fig. 1, bottom). The reason to study this geometry is twofold. First, the surface free energy cost is a key ingredient of the RFOT theory,^{30,35} but little is known about it. The very possibility of measuring the surface tension between amorphous states is at present under debate,³⁶ and recently arguments against the existence of amorphous domain walls (a question which is closely related to the previous one) across the bulk of the glassy liquid have been proposed.³⁴ Moreover, it is not clear if the surface tension in a supercooled liquid is a purely entropic phenomenon or if it also includes an energy part due to the mismatch of different states.

Second, the numerical study of the excess energy provides in principle a method to estimate the stiffness exponent θ , another crucial player in the RFOT formulas, regulating the growth of the correlation length. Unfortunately, we shall see that, although the sandwich geometry is in principle ideal to determine θ through the technique of the aspect ratio scaling, in practice the present values of the correlation length are not large enough to make an unambiguous determination of θ .

A. Interface energy

We define the excess energy as the difference between the extensive energy of the mobile part of the sandwich with “anti-parallel” boundary conditions and “parallel” boundary conditions,

$$\Delta E(d) = E_{\alpha\beta}(d) - E_{\alpha\alpha}, \quad (12)$$

averaged over 16 samples. It is important to note that, if we average over a large enough number of samples, the energy $E_{\alpha\alpha}$ is equal to the (extensive) equilibrium energy. In the anti-parallel case, relaxation of the energy is in general very slow, and it get slower for smaller d . This fact is true even using the accelerated swap dynamics (Fig. 6). Clearly, the system is

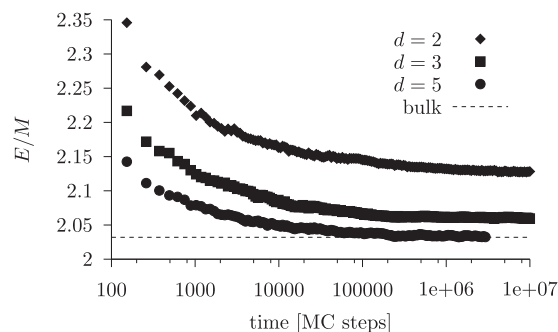


FIG. 6. Excess energy per mobile particle at $T = 0.246$ and several values of d , together with the bulk (PBC) average value.

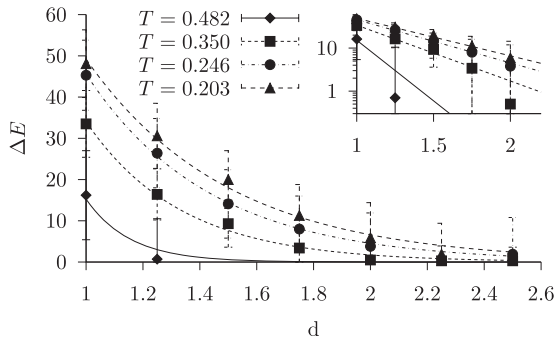


FIG. 7. Excess energy vs. d at several temperatures and $L = 16$. Lines are exponential fits. (Inset) Same data in semilog scale.

unhappy with the $\alpha\beta$ boundary, likely because of the forcing of a domain wall. For this reason, at the smallest values of d we do not reach a plateau of the energy even for our longest time. In these cases, we extrapolate the limiting value of the excess energy by using a power-law fit,

$$\Delta E(t, d) = \Delta E(d) + At^{-\alpha}. \quad (13)$$

Figure 7 shows the excess energy $\Delta E(d)$ for all the values of d studied. As expected, ΔE decays when increasing d , and, at fixed d , the excess energy grows upon lowering the temperature. At the largest temperature $T = 0.482$ though, ΔE is basically always zero except for the smallest d . The fact that the energy cost to match independent amorphous configurations vanishes for high temperatures seems to support the existence of the spinodal crossover proposed in Refs. 37–39.

At the three lowest temperatures, the excess energy seems to be well described by an exponential decay with d ,

$$\Delta E(d) \sim e^{-d/l}, \quad (14)$$

(see inset of Fig. 7). We must note that, at variance with the case of the point-to-set correlation, in the excess energy we do not find any hint of nonexponentiality. Moreover, the decay of $\Delta E(d)$ defines a new lengthscale l . We shall investigate in Sec. VI whether l can be identified with the point-to-set correlation length ξ or with the penetration length λ .

B. Aspect ratio scaling

It is interesting, and potentially useful, to analyze the excess energy using some simple scaling relations, partially inspired by the aspect-ratio-scaling technique introduced in Ref. 40. The basic ideas of this subsection have been already used in the naïve RFOT argument of Sec. V A.

The relevant lengthscales for ΔE are d , l and L , the longitudinal size of the sandwich. The first thing we can say is that the excess energy will scale like a length to the exponent θ (which is basically a definition of the stiffness exponent). Hence,

$$\Delta E \sim YL^\theta f(d/L, l/L), \quad (15)$$

where Y is the (generalized) surface tension. One can choose any of the three lengths to fix the dimensions by appropriately changing the scaling function f . The second requirement is

that the energy and the excess energy must be extensive: in the limit $L \gg d$, the ΔE from different pieces of the surface must add up. This implies that,

$$\Delta E \sim L^2, \quad (16)$$

a relation very well obeyed by our data. For this to be true, we need that

$$f(d/L, d/l) \sim (L/d)^{2-\theta} g(d/l). \quad (17)$$

Moreover, as we have seen from the data, the scale l seems well set by an exponential decay, so it is reasonable to assume $g(x) = e^{-x}$, so that

$$\Delta E(d) \sim YL^2 \frac{1}{d^{2-\theta}} e^{-d/l}. \quad (18)$$

This is an interesting formula, and one could in principle use it to fit the stiffness exponent θ . In particular, the formula suggests that, if a purely exponential fit is satisfactory (as in our case), then $\theta \sim 2$. In practice, the formula is useful to discriminate different values of θ only for large d ; but for ΔE to be nonzero at large d , we need very large values of l , i.e., very low temperatures, which we do not have. In fact, any exponent θ in the interval $[1, 2]$ does an equally good job in fitting our data for $\Delta E(d)$. In particular, distinguishing between $\theta = 3/2$ and $\theta = 2$ is completely out of the question. Yet, the method is conceptually interesting, and future simulations, at lower T , may eventually use it to determine the stiffness exponent.

VI. COMPARISON OF THE DIFFERENT LENGTHSCALES AND THE ISING CASE

Let us summarize the three lengthscales we have measured. The first one is the point-to-set correlation length, ξ , defined as the decay scale of the overlap measured at the center of a sandwich of half-width d ,

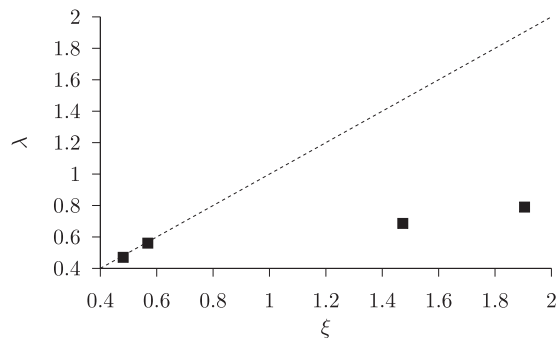
$$q_c(d) \sim \exp[-(d/\xi)^\zeta] + q_0. \quad (19)$$

Previous investigations suggest that this is the true static correlation length of the system, the one relevant for the structural rearrangement.⁴¹ Moreover, there is evidence¹⁹ that ξ has to be identified with the RFOT correlation length, discussed above. The remarkable feature of the point-to-set correlation length is that its associated correlation function has a nonexponential decay at low temperature.

The second lengthscale is the penetration length λ , which regulates the decay of the overlap off a single wall in a semi-infinite geometry,

$$q(z) \sim \exp[-z/\lambda] + q_0. \quad (20)$$

This lengthscale seems to have a different physical meaning than the correlation length ξ , as also suggested in Ref. 32. It seems to embody the extent to which the effect of a single frozen wall penetrates into the system, rather than the average size of a rearranging region. At variance with the point-to-set correlation length, λ regulates a purely exponential decay of the overlap. Regarding the penetration length, there are interesting, although perhaps not compelling, similarities between our results and those of Ref. 42.

FIG. 8. Penetration length λ vs. point-to-set correlation length ξ .

Finally, we measured the lengthscale l associated to the decay in d of the excess energy produced by imposing “anti-parallel” boundary conditions,

$$\Delta E(d) = E_{\alpha\beta} - E_{\alpha\alpha} \sim \exp[-d/l]. \quad (21)$$

As in the case of the penetration length, the excess energy lengthscale l is associated to a purely exponential decay, at least down to our lowest available temperature.

What can be said about the quantitative relationship (if any) between these three lengthscales? We report them all in Table I, together with the anomaly exponent ζ .

One could object that much of the comparison depends on the fitting procedure of the data, which is not a nice thing. This is certainly a concern. However, we notice that extracting the lengthscales by crossing the various functions with arbitrary threshold would not be any better, for two reasons: first, in presence of a nonexponential decay (as $q_c(d)$ unmistakably has), with a T -dependent anomalous exponent ζ , the arbitrary value of the threshold can strongly bias the dependence of ξ on T ; second, these are dimensionally different, inhomogeneous functions, so it would be hard to choose coherently a crossing point for each of them. An honest fit is the best we can do.

From the table, we see that the correlation length ξ is larger than the other two scales. Of course, what really matters is their mutual T -dependence, namely: is there any of them that grows significantly faster than the others, when lowering T ? More precisely, we would like to understand whether or not these lengths are ruled by different exponents. Because of this, comparing the three plots, $\xi(T)$, $\lambda(T)$, $l(T)$, is not a good idea: constant factors would show up as increasing dif-

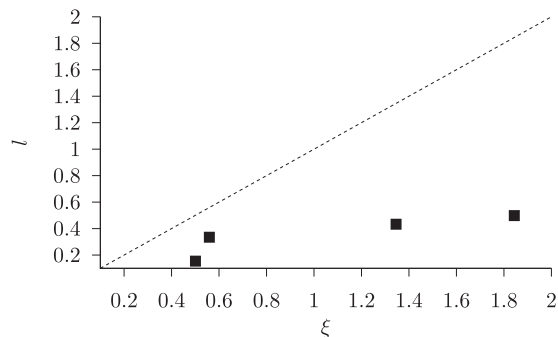
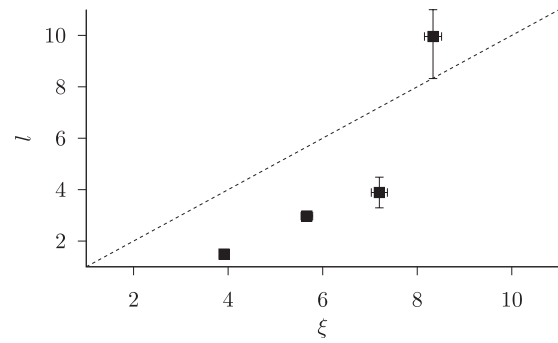
FIG. 9. Energy decay length l vs. point-to-set correlation length ξ .

FIG. 10. Energy decay length vs. two-spin correlation length for the Ising model in the square lattice. Data are from Monte Carlo simulations on a 100×100 lattice with single-flip Metropolis dynamics performed above the critical point, at temperatures $T = 2.5J$, $T = 2.4J$, $T = 2.35J$ and $T = 2.32J$, where J is the Ising coupling constant (the critical point is $T_c \approx 2.269J$). The correlation length was obtained from a fit of the spin-spin space correlation function $C(r) = \langle S(0)S(r) \rangle$. To determine the length l , sandwich configurations were prepared as explained for the liquid case, measuring the excess energy $\Delta E(d) = E_{\alpha\beta} - E_{\alpha\alpha}$ for $d = 1, 2, 3, 4, 5, 7.5, 10, 15, 20, 25$ and 45 lattice spacings, and fitting to an exponential decay.

ferences, conveying the (wrong) idea that one length is growing faster than the other. The best thing to do is to plot one lengthscale vs. the other, parametrically in T . This is what we do in Figs. 8 and 9.

The result of this comparison is unfortunately not conclusive. Even though, as we already said, the correlation length ξ is larger than the other two, all mutual dependencies are not far from linear. This means that, with such data, we cannot claim that ξ is growing with an exponent significantly different from the other two, which would be the only proof of a qualitative difference between these scales. Of course, our data do not either rule this out.

In such a murky situation, some conceptual help may perhaps come from the well-known Ising model. There one can use (true) anti-parallel boundary conditions to force a domain wall (below the critical temperature T_c). Then there is a finite surface tension and the excess free energy (anti-parallel minus parallel) in the limit $d \rightarrow \infty$ tends to the finite value σL^{d-1} , where σ is the surface tension. For $T > T_c$, one can instead impose (similar to what we have done above) two different paramagnetic configurations on the two sides of the sandwich and measure the excess energy. In this case, we expect the excess energy to decay to zero for large d , but on what scale does this happen? Simulations in two-dimensions show that the excess energy decays exponentially with a lengthscale l , which we can compare with the Ising correlation length ξ , calculated from the standard spin-spin space correlation function. Data show that l and ξ scale linearly with each other (parametrically in T , Fig. 10), though l is somewhat 2 smaller than ξ . Therefore, in Ising, correlation decay and excess energy decay seem to track each other quite closely.

VII. CONCLUSIONS

We have studied the point-to-set correlation function in a linear (sandwich) geometry, with different kinds of boundary conditions. This has allowed us to define several growing lengthscales and to study their mutual relationships. Before

summarizing and commenting our results, let us mention that Szamel and Flenner in a recent work⁴³ have raised some warnings about interpreting the point-to-set correlation length in a geometry different from the present one, the so-called random pinning geometry.⁴⁴ The point of Ref. 43 is that much of the signal one observes in the correlation function has a trivial origin and it should not be associated with any many-body correlations. We are unable to judge whether this argument applies also to the sandwich geometry we study here, but it seems fair to make the reader aware of this warning.

Similar to what we found in the spherical geometry,¹⁹ the sandwich data show a crossover from exponential to non-exponential relaxation of the point-to-set correlation function, upon lowering the temperature. We remark that such crossover is one of the very few (if not the only one) static landmarks differentiating at the qualitative level the fluid phase from the deeply supercooled phase in glass-forming liquids. Having found this feature now in two different geometries makes it quite a robust phenomenon.

Up to now, the only reasonable explanation of such sharper-than-exponential relaxation has been given in the context of RFOT. However, the point-to-set construction will pick up correlations and measure correlation length even in system that are not ruled by RFOT. An obvious example is the simple Ising model, where the point-to-set measures the standard, very much non-RFOT, correlation length.⁴⁵ Moreover, even in glassy systems the situation may be complicated: a nontrivial point-to-set correlation length has been detected in the kinetically constrained models studied in Refs. 46 and 47 where RFOT is certainly not at work. In fact, we think that this adds to the relevance of the point-to-set construction as tool of investigation. Moreover, even in more standard glass-formers, as the one studied here, if one freezes the fixed particles in a random (infinite T) configuration, as recently done in Ref. 48, one will certainly detect a (growing) lengthscale, which is not necessarily ruled by a RFOT scenario (although it may be related to it). For all these reasons, we believe that accompanying the observation of a growing correlation length with an equally growing nonexponential behaviour is the most important landmark we find of some RFOT signature.

We reported a naïve RFOT argument for the sandwich and showed that there should be no essential variations (at least in three dimensions) with respect to the standard argument one uses in the cavity geometry. Our sandwich results therefore give further support to the theoretical connection between point-to-set nonexponential relaxation and RFOT.

A more thorough formulation of the RFOT argument, based on a renormalization group framework, could turn the nonexponential, but smooth, drop of the overlap at $d = d_{\text{RFOT}}$, into a true transition, in the limit $L \rightarrow \infty$.³² The very existence of such limit would be one of the main benefits of the sandwich vs. the cavity geometry. However, this transition is supposed to be smeared out by disorder (surface tension fluctuations) in a three-dimensional sandwich,³² and indeed, by substantially increasing L , we do not find any relevant change in the point-to-set correlation function.

A different experiment consists in measuring the overlap decay off a single wall. In this case, we found a

behaviour rather different from the point-to-set correlation function. First, and most important, this decay is purely exponential, even at the lowest temperature studied, where the point-to-set correlation function is clearly nonexponential. Hence, the single wall seems less than ideal to characterize at the qualitative level the deeply supercooled phase.

Second, the lengthscale of this single-wall decay, i.e., the penetration length λ , seems to be smaller than the point-to-set correlation length, ξ . According to Ref. 49, both ξ and λ should diverge at T_k , but with different exponents, in particular the divergence of ξ should be sharper than that of λ . This is due to the fact that λ is not controlled by the RFOT entropy vs. surface tension competition mechanism so directly as ξ is. Even though we are far (to say the least) from the $T \sim T_k$ region where the RG arguments of Ref. 49 hold, we can at least say that our numerical data are not in contradiction with this scenario. We should however point out that the recent RG analysis of Ref. 50 is in disagreement with the results of Ref. 49.

We used “anti-parallel” boundary conditions in the sandwich to measure the excess energy associated to an interface. This quantity seems to decay purely exponentially with the half-width d of the sandwich, over a lengthscale l that grows by lowering the temperature. Unfortunately, the value of l we obtain even at the lowest T is not large enough to make it possible an estimate of the stiffness exponent θ using aspect ratio scaling. However, the technique seems promising in this context, and perhaps future simulation will reach a regime able to discriminate between different (theoretical) values of θ .

An obvious question is whether and how the lengthscale of the excess energy l is related to the other two lengthscales, and in particular to the correlation length, ξ . We do not have a final answer to this question. Even though ξ seems to be quantitatively larger than l (about a factor 4), there is no clear evidence of a nonlinear connection between the two lengths. On one hand, by following an economy criterion, we are tempted to conclude that point-to-set and excess energy are regulated by one lengthscale, as it happens in the Ising model above T_c . On the other hand, the very different kind of relaxation (nonexponential for the point-to-set correlation function, exponential for the excess energy), and the fact that l is significantly smaller than ξ , seem to suggest otherwise. We cannot but leave the question open.

Finally, the Ising example calls for caution in the interpretation of our results about the excess energy. The fact that in a purely paramagnetic state one finds a behaviour of ΔE vs. d so similar to the glass-forming case, means that a finite ΔE is not by itself proof of the existence of a surface tension. This calls for a thorough investigation of the possible entropic contribution to the glassy surface tension (which we do not measure here).

ACKNOWLEDGMENTS

We warmly thank Giorgio Parisi for making us familiar with the aspect ratio scaling technique. We also thank Giulio Biroli and Chiara Cammarota for several important discussions. T.S.G. thanks the Dipartimento di Fisica of the

Sapienza Università di Roma and ISC (CNR, Rome) for hospitality. The work of G.G. is supported by the “Granular-Chaos” project, funded by Italian MIUR under the Grant No. RBID08Z9JE. PV was partly supported by MICINN (Spain) through Research Contract Nos. FIS2009-12648-C03-01 and FIS2008-01323 (PV). T.S.G. was partially supported by ANPCyT (Argentina).

- ¹H. Sillescu, *J. Non-Cryst. Solids* **243**, 81 (1999).
- ²M. D. Ediger, *Annu. Rev. Phys. Chem.* **51**, 99 (2000).
- ³E. Vidal-Russell and N. E. Israeloff, *Nature (London)* **408**, 695 (2000).
- ⁴L. Berthier and J. P. Garrahan, *J. Chem. Phys.* **119**, 4367 (2003).
- ⁵H. E. Castillo, C. Chamon, L. F. Cugliandolo, J. L. Iguain, and M. P. Kennett, *Phys. Rev. B* **68**, 134442 (2003).
- ⁶L. Berthier, *Phys. Rev. Lett.* **91**, 055701 (2003).
- ⁷L. Berthier, *Phys. Rev. E* **69**, 020201 (2004).
- ⁸H. Sillescu, R. Böhmer, G. Diezemann, and G. Hinze, *J. Non-Cryst. Solids* **307-310**, 16 (2002).
- ⁹J. P. Garrahan and D. Chandler, *Phys. Rev. Lett.* **89**, 035704 (2002).
- ¹⁰L. Berthier, G. Biroli, J.-P. Bouchaud, L. Cipelletti, D. E. Masri, D. L’Hôte, F. Ladieu, and M. Pierno, *Science* **310**, 1797 (2005).
- ¹¹L. Berthier, G. Biroli, J.-P. Bouchaud, W. Kob, K. Miyazaki, and D. R. Reichman, *J. Chem. Phys.* **126**, 184503 (2007).
- ¹²L. Berthier, G. Biroli, J.-P. Bouchaud, W. Kob, K. Miyazaki, and D. R. Reichman, *J. Chem. Phys.* **126**, 184504 (2007).
- ¹³D. Kivelson, G. Tarjus, and S. A. Kivelson, *Prog. Theor. Phys. Supp.* **126**, 289 (1997).
- ¹⁴A. Cavagna, T. S. Grigera, and P. Verrocchio, *Phys. Rev. Lett.* **98**, 187801 (2007).
- ¹⁵A. Widmer-Cooper, H. Perry, P. Harrowell, and D. R. Reichman, *Nat. Phys.* **4**, 711 (2008).
- ¹⁶H. Tanaka, T. Kawasaki, H. Shintani, and K. Watanabe, *Nature Mater.* **9**, 324 (2010).
- ¹⁷D. Coslovich, *Phys. Rev. E* **83**, 051505 (2011).
- ¹⁸P. Scheidler, W. Kob, K. Binder, and G. Parisi, *Philos. Mag. B* **82**, 283 (2002).
- ¹⁹G. Biroli, J.-P. Bouchaud, A. Cavagna, T. S. Grigera, and P. Verrocchio, *Nat. Phys.* **4**, 771 (2008).
- ²⁰L. Berthier and W. Kob, *Phys. Rev. E* **85**, 011102 (2012).
- ²¹W. Kob, S. Roldán-Vargas, and L. Berthier, *Nat. Phys.* **8**, 164 (2012).
- ²²G. M. Hocky, T. E. Markland, and D. R. Reichman, *Phys. Rev. Lett.* **108**, 225506 (2012).
- ²³A. Montanari and G. Semerjian, *J. Stat. Phys.* **125**, 23 (2006).
- ²⁴E. Zarinelli and S. Franz, *J. Stat. Mech.: Theory Exp.* **2010**, P04008.
- ²⁵B. Bernu, J. P. Hansen, Y. Hiwatari, and G. Pastore, *Phys. Rev. A* **36**, 4891 (1987).
- ²⁶T. S. Grigera and G. Parisi, *Phys. Rev. E* **63**, 045102 (2001).
- ²⁷Y. Brumer and D. R. Reichman, *Phys. Rev. E* **69**, 041202 (2004).
- ²⁸T. R. Kirkpatrick and P. G. Wolynes, *Phys. Rev. B* **36**, 8552 (1987).
- ²⁹T. R. Kirkpatrick and D. Thirumalai, *Phys. Rev. B* **37**(10), 5342 (1988).
- ³⁰J.-P. Bouchaud and G. Biroli, *J. Chem. Phys.* **121**, 7347 (2004).
- ³¹C. Cammarota and G. Biroli, private communication (2012).
- ³²C. Cammarota and G. Biroli, *Proc. Natl. Acad. Sci. U.S.A.* **109**, 8850 (2012).
- ³³J. Kurchan and D. Levine, *J. Phys. A: Math. Theor.* **44**, 035001 (2011).
- ³⁴C. Cammarota and G. Biroli, *Europhys. Lett.* **98**, 36005 (2012).
- ³⁵T. Kirkpatrick, D. Thirumalai, and P. Wolynes, *Phys. Rev. A* **40**, 1045 (1989).
- ³⁶S. Franz and G. Semerjian, “Analytical approaches to time- and length scales in models of glasses,” in *Dynamical Heterogeneities in Glasses, Colloids, and Granular Media*, edited by L. Berthier, G. Biroli, J.-P. Bouchaud, L. Cipelletti, and W. van Saarloos (Oxford University Press, 2011); [arXiv:1009.5248](https://arxiv.org/abs/1009.5248) [cond-mat.stat-mech].
- ³⁷C. Cammarota, A. Cavagna, G. Gradenigo, T. S. Grigera, and P. Verrocchio, *J. Stat. Mech.: Theory Exp.* **2009**, L12002.
- ³⁸C. Cammarota, A. Cavagna, G. Gradenigo, T. S. Grigera, and P. Verrocchio, *J. Chem. Phys.* **131**, 194901 (2009).
- ³⁹C. Cammarota, A. Cavagna, I. Giardina, G. Gradenigo, T. S. Grigera, G. Parisi, and P. Verrocchio, *Phys. Rev. Lett.* **105**, 055703 (2010).
- ⁴⁰A. Carter, A. Bray, and M. Moore, *Phys. Rev. Lett.* **88**, 077201 (2002).
- ⁴¹A. Cavagna, T. S. Grigera, and P. Verrocchio, *J. Chem. Phys.* **136**, 204502 (2012).
- ⁴²K. Watanabe, T. Kawasaki, and H. Tanaka, *Nature Mater.* **10**, 512 (2011).
- ⁴³G. Szamel and E. Fleener, “Glassy dynamics of partially pinned fluids: an alternative mode-coupling approach,” e-print [arXiv:1204.6300](https://arxiv.org/abs/1204.6300).
- ⁴⁴K. Kim, *Europhys. Lett.* **61**, 790 (2003).
- ⁴⁵C. Cammarota and A. Cavagna, *J. Chem. Phys.* **127**, 214703 (2007).
- ⁴⁶R. L. Jack and J. P. Garrahan, *J. Chem. Phys.* **123**, 164508 (2005).
- ⁴⁷R. L. Jack and L. Berthier, *Phys. Rev. E* **85**, 021120 (2012).
- ⁴⁸S. Karmakar and G. Parisi, e-print [arXiv:1208.3181](https://arxiv.org/abs/1208.3181).
- ⁴⁹C. Cammarota, G. Biroli, M. Tarzia, and G. Tarjus, *Phys. Rev. Lett.* **106**, 115705 (2011).
- ⁵⁰J. Yeo and M. A. Moore, *Phys. Rev. B* **85**, 100405 (2012).